

Bone and Skin Tissue Engineering based on Cytotoxicity Assays of PLLA Fibrous Mats Synthesized via Centrifugal Spinning

BÁRBARA ETRURI CIOCCA¹

National Institute of Biofabrication, University of Campinas
Campinas, Sao Paulo, Brazil

School of Chemical Engineering, University of Campinas
Campinas, Sao Paulo, Brazil

NAHIEH TOSCANO MIRANDA

School of Chemical Engineering, University of Campinas
Campinas, Sao Paulo, Brazil

GUINEA BRASIL CAMARGO CARDOSO

ANA AMÉLIA RODRIGUES

ANA FLÁVIA PATTARO

National Institute of Biofabrication, University of Campinas
Campinas, Sao Paulo, Brazil

ANDRÉ LUIZ JARDINI MUNHOZ

RUBENS MACIEL FILHO

National Institute of Biofabrication, University of Campinas
Campinas, Sao Paulo, Brazil

School of Chemical Engineering, University of Campinas
Campinas, Sao Paulo, Brazil

Abstract

Poly (L-lactic acid) (PLLA) is a biocompatible polymer widely used in a range of applications and is already recognized in the medical field as a biomaterial. The main objective of the present work was the production of polymeric mats to be applied in tissue engineering. PLLA mats were produced through the centrifugal spinning process. Scanning electron microscopy (SEM) analyzed the

¹ Corresponding author: barbara_ciocca@hotmail.com

fibers diameter, disposition, and morphology. The fibers presented a uniform and constant diameter (16.24 μm), being arranged randomly. Thermogravimetric analysis (TGA) technique verified variation of mass loss with temperature, in which the material degradation temperature started at 205 °C. Differential scanning calorimetry (DSC) determined phase transition temperatures. Fourier-transform infrared spectroscopy (FT-IR) evaluated PLLA fibrous membrane chemical groups. Cytotoxicity assays verified fibroblasts and osteoblasts viabilities by MTT (3-(4,5-Dimethylthiazol-2-yl)-2,5-Diphenyltetrazolium Bromide), AlamarBlue®, and Live/Dead® for 24, 48, and 72 h. This work results demonstrated that PLLA mats have great potential for tissue engineering applications in wound healing and bone repairing, being a promising biomaterial with high biocompatibility.

Key words: PLLA; centrifugal spinning; tissue engineering; biomaterial; biocompatibility.

1. INTRODUCTION

Tissue engineering currently uses several types of materials, such as metals, ceramics, composites, and polymers. The material selection depends on the application site of the body. Poly (L-lactic acid) (PLLA) has received widespread approval in the medical field for being cytocompatible and biodegradable, making it an ideal candidate for implantable devices [1,2]. Besides PLLA presents several other desirable characteristics such as biodegradable, possessing favorable aspects on the processability, the formulation flexibility, the excellent structural properties, and the low cost compared to available conventional materials [3,4].

PLLA fibrous mats are particularly well suited to address healing. The fibrous meshes mimic the native topography of the body tissues and assist in protecting the wound bed, preventing loss of moisture and proteins, and removal of exudate [5,6]. The large surface area-to-volume ratio of nanofibrous meshes also encourages the attachment and proliferation of cells, promoting the closure of large

wounds. [6]. In the area of skin regeneration, PLA is particularly useful because nanofibrous mats can be leveraged as drug delivery vehicles as well as providing a hydrophobic barrier against water loss and the environment. Scaffolds for bone tissue engineering are typically fabricated with low surface area to volume ratio geometries, usually cylinders, which provide mechanical stability and an environment conducive to bone regeneration [7,8].

The use of centrifugal spun mats has considerably grown due to diverse application possibilities in the medical field, such as artificial skin production for wounds healing, angioplasty balloons, intragastric balloons, scaffolds, neural connections, among others [3].

Currently, to obtain fibers and mats are used two methods directly competing; centrifugal spinning process and electrospinning. In the electrospinning, several parameters controls are needed, such as the thickness of the needle, the distance between the needle and the collector, and the high voltage to be used, besides production speed are very slow, whereas in centrifugal spinning process the speed of the equipment [9]. Centrifugal spinning process is a fast and simple method of obtaining fibers with great potential to be applied on industrial scale [10].

It is important to note that there is a shortage of information in the literature regarding the lack of biological assays with PLLA mats obtained by centrifugal spinning process to confirm the possibility of using these fibers in the medical field. In this way, the purpose of this study was to prepare PLLA mats via the centrifugal spinning process and to characterize them regarding morphology, thermal properties, chemical structure, and *in vitro* cell viability.

2. MATERIALS AND METHODS

The research group of the National Institute of Biofabrication (INCT-Biofabris/UNICAMP) provided the PLLA, and PATTARO (2016) [11] describes its synthesis.

2.1.1. PLLA Solution Preparation

PLLA solution was dissolved in chloroform [CHCl_3 , 99.0 % from Synth] at a concentration of 0.2 % (w/v), at room temperature for 24 h.

2.1.2. Centrifugal Spun PLLA Mats Preparation

The Laboratory of Biomaterials and Biomechanics (LABIOME/UNICAMP) designed and developed the centrifugal spinning device. It consists of a central vessel with four small orifices in the wall, a collector, and a base coupled to a motor.

With a syringe, the central hole continuously collects the polymeric solution at room temperature and speed of 6,500 RPM.

2.1.3. Fibroblasts cell culture

The Adolfo Lutz Institute (Sao Paulo, Brazil) donated VERO cells (derived from African Green Monkey kidney fibroblasts). The cells were cultured in low-glucose Dulbecco's Modification of Eagle's Medium (DMEM-LG – Gibco/Thermo Fisher, Waltham, MA, USA), supplemented by 10.0 wt% of fetal bovine serum (FBS) and 1.0 wt% of penicillin and streptomycin (PS) (both from Gibco). The cells were maintained at 37 °C in an incubator (Sanyo Electric Biomedical, Osaka, Japan) with an atmosphere with 5.0 % of CO₂ and 95.0 % of ambient air. DMEM-LG with phenol (10.0 wt%) was the positive control for toxicity (PCT), whereas DMEM-LG with FBS (10.0 %) and PS (1.0 wt%) was the negative control for toxicity (NCT).

2.1.4. Osteoblasts cell culture

We purchased osteoblastic cell line M3CT3-E1 from ATCC, Manassas, VA, USA. The cells were cultured in Eagle's Minimum Essential Medium (α -MEM – Vitrocell, Campinas, Brazil), supplemented with 10.0 wt% of fetal bovine serum (FBS) and 1.0 wt% of penicillin and streptomycin (PS) (both from Gibco). The procedure was the same as previously described (see section 2.1.3).

2.2 PLLA mats characterization

2.2.1. Morphological characterization

Scanning electron microscopy (SEM) technique provided the sample surface morphological analysis, using LEO – scanning electron microscope (Oxford, Leo 440i, Cambridge, England), with a voltage of 20 kV and a current of 100 pA. The sample went through a metallic coating process with gold on a metallizer (SputterCoater EMITECH, K450, Kent, UK). *ImageJ* software determined 100 fibers sizes using the SEM data. The fiber size was the arithmetic mean of the achieved values.

2.2.2. Thermal characterization

Thermogravimetric analysis (TGA) (METTLER TOLEDO, TGA/DSC1 Schwerzenbach, Switzerland) verified the material thermal degradation. We weighed about 10 mg of the sample on a microanalytical balance (Mettler Toledo, MX5, Schwerzenbach, Switzerland) and placed in a 70 μL alumina crucible. It was heated under an inert nitrogen atmosphere (50 mL/min) from 25 to 450 $^{\circ}\text{C}$, at a heating rate of 10 $^{\circ}\text{C}/\text{min}$.

Differential scanning calorimetry (DSC) analysis verified the material phase transition temperatures via calorimeter (Mettler Toledo DSC 823^e). The measurements used a nitrogen atmosphere (50 mL/min), with temperatures ranging from 25 to 200 $^{\circ}\text{C}$, at a heating rate of 10 $^{\circ}\text{C}/\text{min}$. A 40 μL aluminum crucible placed 7 mg of sample. We heated the material at 200 $^{\circ}\text{C}$, below its degradation temperature. Then, it cooled to 25 $^{\circ}\text{C}$ and heated again to 200 $^{\circ}\text{C}$. This process makes the material to lose its thermal memory. The second heating step represents the behavior of the membrane without processing impact.

2.2.3. Chemical structures characterization

Fourier-transform infrared spectroscopy (FT-IR) (Nicolet 6700 FT-IR Spectrophotometer) with an Attenuated Total Reflection - ATR (Smart Omni Sampler) (both from ThermoScientific, Madison/USA) evaluated the fibrous membrane chemical groups. The sample was scanned 128 times in 675 to 4000 cm^{-1} range of wavenumbers, using a resolution of 4 cm^{-1} , at ambient atmosphere and room temperature.

2.2.4. In vitro cell viability evaluation

The direct cytotoxicity of fibroblasts and osteoblasts on the spun mats was determined by seeding the cells onto 96-well culture plates (Corning Inc, Corning, USA) at 1×10^6 cells/mL for MTT and AlmarBlue[®] assays, and at 1×10^3 cells/mL for Live/Dead[®] assays. Then, we incubated the cells for 24, 48, and 72 h, in contact with centrifugal spun PLLA mats.

For MTT, we incubated the cells for 04 h with MTT solution dissolved in 200 μL of cell culture medium. The optical density of viable cells was read through an absorbance reading in a microplate reader (Microplate Reader F5, Molecular Probes, Eugene, OR, EUA) at a wavelength of 595 nm.

For AlamarBlue®, we first removed the medium and then added 50 µL of AlamarBlue® reagent solution to the wells (manufacturer recommendations). The fluorescence filters at 460 nm (emission) and 630 nm (excitation) detected the presence of viable cells in a microplate reader.

We submitted the results of AlamarBlue® and MTT assays to a normality test (Shapiro-Wilk). Subsequently, we performed an analysis of variance (ANOVA) and Tukey's test. The results are the mean value with standard deviation, and the significance level was 0.05. We used the software PAST (Oslo, Norway) for the statistical analyses.

Live/Dead® assay kit (Live/Dead® kit, Gibco) checked fibroblasts and osteoblasts viability (manufacturer recommendations). We incubated the cells in a solution, which contains 02 µM of propidium iodide and 02 µM of calcein AM solution, for 30 min at 37 °C to stain viable and non-viable cells to obtain fluorescence microscopy images.

3. RESULTS

3.1. Morphological evaluation

SEM provided the centrifugal spun PLLA membrane fibers morphology. The produced membrane (Fig. 1) are scattered and overlapped in a disorderly manner. The images demonstrate the fibers do not present pores and beads, having a smooth surface and constant diameter due to the solution optimal concentration in the centrifugal spinning process and to the solvent evaporation characteristics.

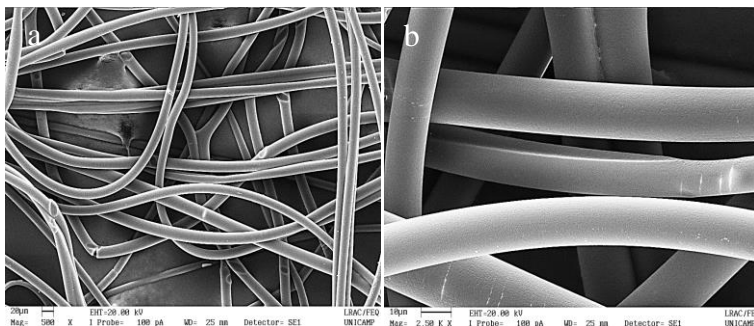


Figure 1 – SEM images of the centrifugal spun PLLA membrane fibers in 20 µm (a) and 10 µm (b).

The histogram (Fig. 2) shows the distribution and frequency of fiber sizes, in which the Gaussian curve demonstrates how the diameters normal distribution are close to the average value, which is approximately 16.24 μm . The fibers most significant amount is in the midpoint, in which about 72.0 % of their diameters are between 13 to 19 μm .

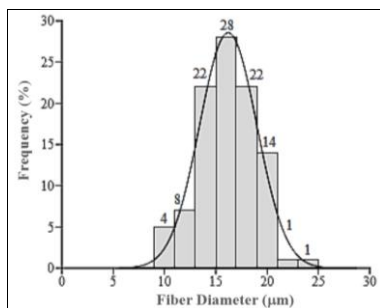


Figure 2 – Histogram of the centrifugal spun PLLA fibers diameters distribution.

3.2. Thermal analysis using TGA and DSC

The variation of PLLA mass loss with the temperature (TGA) (Fig. 3) determined its thermal degradation process.

The TGA curve shows only one step of mass loss, which happened at approximately 205 $^{\circ}\text{C}$ (T_i – initial temperature), representing the material degradation was fast. It reaches the final degradation temperature (T_f) at 285 $^{\circ}\text{C}$, indicating the PLLA membrane completed degradation. Through the curve derivative, we found the acceleration of degradation temperature of the material is 245 $^{\circ}\text{C}$.

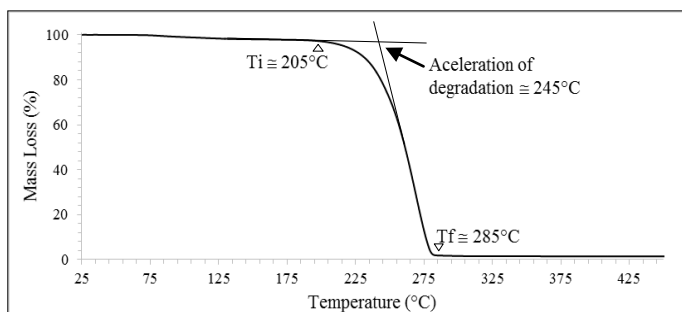


Figure 3 – TGA of PLLA membrane.

DSC thermogram (Fig. 4) demonstrated the phase transition temperatures in the centrifugal spun PLLA membrane, referring to the first and second heating processes. The diagram enabled the determination of the following temperatures: the glass transition (T_g), the initial crystallization (T_c), the cold crystallization (T_{cc}), and the melting (T_m).

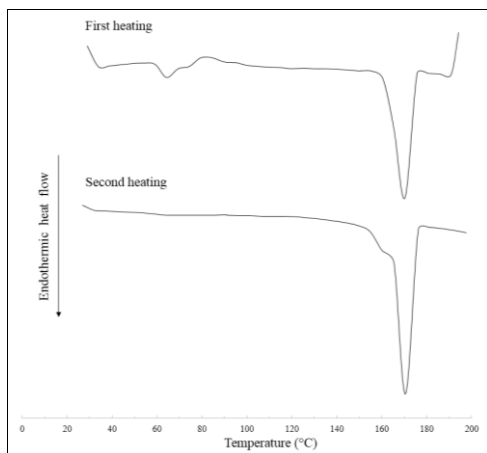


Figure 4 – DSC thermogram of PLLA membrane.

The PLLA membrane T_g , T_c , T_{cc} , and T_m appears in the first heating process, but only T_m arises in the second heating process. Also, there is a well-defined peak in the first heating, whereas a bimodal region becomes evident in the second heating.

T_g happens at 63 °C, in which the polymeric chains movement begins, changing their shape. T_c occurs at approximately 73 °C and T_{cc} at 80 °C, in which a point crystalline structure formation happens through polymeric chains movement. T_m is about 173.5 °C in the first heating, while two new crystalline phases in its structure occur in the second heating: the first at about 160 °C and the second one at 170 °C, in which the polymeric chain crystalline regions disappear and melt, leaving the polymer in a molten state.

3.3. PLLA chemical constitution analysis

The FT-IR spectrum (Fig. 5) confirmed the presence of particular PLLA groups and the total solvent exclusion during the centrifugal spinning process.

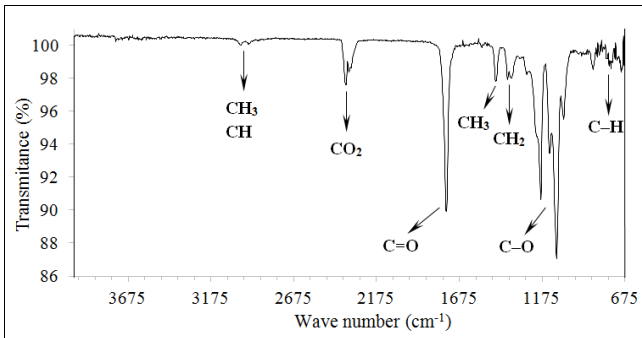


Figure 5 – FT-IR spectra of PLLA mats.

Signals in the range of 3000–2775 cm^{-1} present some slight absorptions related to CH_3 and CH group connections (7, 5, 8). The signal at 1775 cm^{-1} represents the $\text{C}=\text{O}$ group (7, 5, 8). The signals at 1475–1275 cm^{-1} relate to CH_3 and CH_2 groups (7, 5, 8). The highest clear signal referring to the $\text{C}-\text{O}$ group appears at 1175–975 cm^{-1} (7, 5, 8). Finally, the $\text{C}-\text{H}$ group seems to be in the range of 800–675 cm^{-1} (7, 5, 8). The signals at 2375–2275 cm^{-1} refer to the CO_2 interference from the environment due to ATR. No signals appeared in 4000–3000 cm^{-1} , which indicates the sample was moisture free.

3.4. MTT and AlamarBlue® assays

The cytotoxicity assays assess the centrifugal spun PLLA mats biocompatibility. Fibroblasts and osteoblasts were in contact with PLLA mats for 24, 48, and 72 h. Then, we performed the MTT and AlamarBlue® assays to verify the viable cells in contact with PLLA and their controls (PCT and NCT) (Fig. 6).

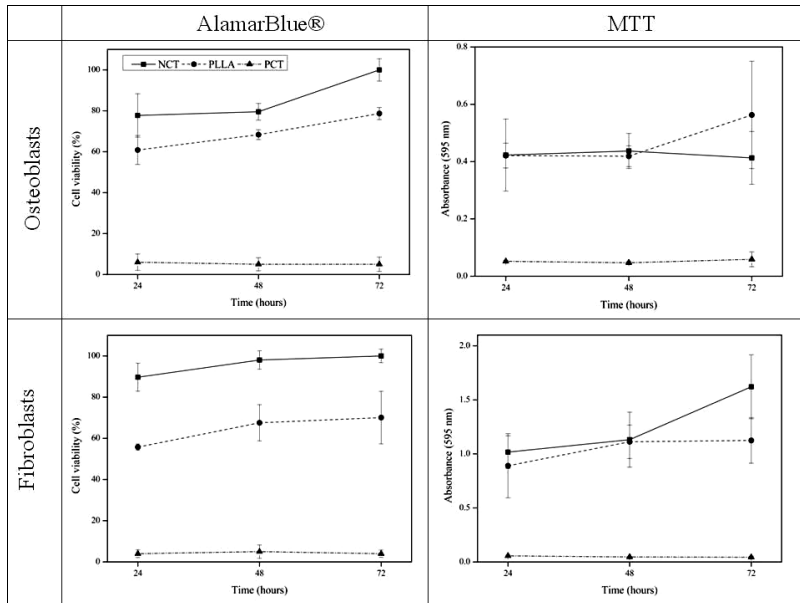


Figure 6 – Cell viability monitored by MTT and AlamarBlue® assays following 24, 48, and 72 h exposure of fibroblasts and osteoblasts cells.

According to the Shapiro-Wilk test, all data follow normality ($p > 0.05$). From ANOVA, the difference between the groups was statistically significant ($p < 0.05$) for cell viability. Tukey's test for MTT assays for fibroblasts and osteoblasts in 24, 48, and 72 h confirmed that there were differences when comparing PLLA with PCT, and NCT with PCT ($p < 0.05$), demonstrating that PLLA is similar to NCT. On the other hand, in AlamarBlue® assay for fibroblasts, we noticed that all groups in 24, 48, and 72 h were different ($p < 0.05$), representing an intermediate behavior between PLLA and controls. For osteoblasts, the only statistical difference occurred when we compared PCT with NCT in 24 h, whereas all other groups presented differences in 48 and 72 h ($p < 0.05$). PLLA expressed an intermediate behavior after 24 h.

3.5. Live/Dead® assays

We determined the PLLA cell viability and toxicity after 24, 48, and 72 h of contact by the Live/Dead® assay kit. Fluorescence microscopy images (Fig. 7) demonstrate viable cells (stained green) and dead cells

(stained red). After this period of contact between PLLA mats and two cell lines, we removed the PLLA.

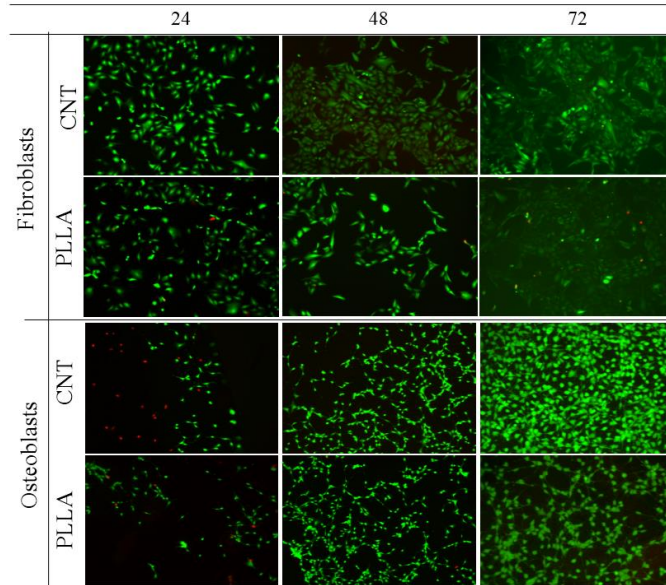


Figure 7 – Live/Dead® assays of fibroblasts and osteoblasts in contact with PLLA mats after 24, 48, and 72 h, and the negative control of toxicity. Amplification: 20x.

Most of the cells were alive (green), both for fibroblasts and osteoblasts. MTT and AlamarBlue® assays also confirmed these results. The results suggest that PLLA mats did not compromise cell viability nor nutrient and oxygen transport to the cells, given the fact that the images of the Live/Dead® assays are akin to the NCT.

4. DISCUSSION

Centrifugal spinning process is a low-cost and simple method to obtain polymeric mats, providing oriented or disordered fibers from micro to nanometric scale. Furthermore, small solution amount can produce large quantities of fibers. In this study, we obtained PLLA fibrous mats through a centrifugal spinning process. The process created uniform surface fibers and presented homogeneous diameters due to the optimal concentration found for the polymeric solution – 0.2

% (w/v). The arranged fibers formed a porous surface membrane, which is suitable for cell attachment. [12–15].

Centrifugal spun PLLA mats have a high thermal capacity to be used as a biomaterial since their degradation temperature starts at approximately 205 °C. It confirms the material does not undergo drastic changes upon implantation, once the body temperature is around 37 °C. Comparing the values of T_m in the second heating (160 °C and 170 °C) with PATTARO (2016) [11] (148.5 °C), we verified that there was variation in the polymer structure of the fibrous membrane due to the centrifugal spinning process of the material.

The FT-IR analysis proved that there are no harmful compounds or chemical bonds to human health. This analysis showed that all chemical bonds are entirely from the polymer structure, confirming total solvent exclusion and no catalyst adherence into the material structure [16].

For fibroblasts MTT and AlamarBlue® assays, PCT behavior had low cell viability in the three analyzed times (24, 48, and 72 h), confirming the death of these cells. NCT had a gradual increase from 24 to 72 h because the cells were alive. The cells in contact with PLLA had an increase from 24 to 48 h and had a steady growth from 48 to 72 h. PLLA proliferation curve behavior seems to be the NCT, in which the centrifugal spun mats are not toxic to cells, indicating the tissue engineering can use this material.

In osteoblasts MTT assay, PCT had low cell viability, and NCT remained constant over the entire trial period. However, the growth of cells in contact with the centrifugal spun PLLA remained similar to NCT from 24 to 48 h and increased from 48 to 72 h. On the other hand, in osteoblasts AlamarBlue® assay, PCT remained constant over the entire trial period, and NCT only demonstrated a significant growth from 48 h. The centrifugal spun PLLA membrane increased throughout the test period. The difference between the tests results is due to AlamarBlue® being more sensitive than MTT [17].

Comparing Live/Dead® assays of both cells, CNT and PLLA present a similarity over the entire test, in which the number of live cells (green) is expressively greater than the dead cells (red). In this way, we concluded the centrifugal spun PLLA mats are not toxic to the cells, assuming its potential to use in tissue engineering.

5. CONCLUSION

We produced PLLA mats through a centrifugal spinning process with optimal polymeric solution concentration. The morphological evaluation demonstrated fibers arrangement in a disorderly manner, with a constant fiber diameter of roughly 16.24 μm . Thermal analyses exhibited high thermal capacity, ideal for tissue engineering applications considering human body temperature (37 °C). The chemical constitution analysis confirmed the successful PLLA synthesis and total solvent exclusion, not demonstrating toxicity.

The biological assays and the statistical analyses confirmed the PLLA mats were capable of maintaining the fibroblasts and osteoblasts functions, not presenting cytotoxicity.

Centrifugal spinning technique combined with synthesized PLLA ensured to be valid on mats production with a suitable porous surface, ideal for cellular proliferation and vascularization, allowing the exchange of essential elements and metabolic products.

This study supports a more thorough investigation of centrifugal spun PLLA mats for many applications in tissue engineering and more in-depth biological studies.

Acknowledgments

The authors are grateful for the financial support provided by CAPES, grant #2008/57680-3, São Paulo Research Foundation (FAPESP), and the National Institute of Biofabrication (INCT-Biofabris).

REFERENCES

- [1] A.J.R. Lasprilla, G.A.R. Martinez, B.H. Lunelli, A.L. Jardini, R. Maciel Filho, Poly-lactic acid synthesis for application in biomedical devices — A review, *Biotechnol. Adv.* 30 (2012) 321–328. doi:10.1016/J.BIOTECHADV.2011.06.019.
- [2] S.T. Lovald, T. Khraishi, J. Wagner, B. Baack, Mechanical Design Optimization of Bioabsorbable Fixation Devices for Bone Fractures, *J. Craniofac. Surg.* 20 (2009). https://journals.lww.com/jcraniofacialsurgery/Fulltext/2009/03000/Mechanical_Design_Optimization_of_Bioabsorbable.25.aspx.

- [3] Y. Zhang, T.L. Chwee, S. Ramakrishna, Z.M. Huang, Recent development of polymer nanofibers for biomedical and biotechnological applications, *J. Mater. Sci. Mater. Med.* 16 (2005) 933–946. doi:10.1007/s10856-005-4428-x.
- [4] K. Pongtanayut, C. Thongpin, O. Santawitee, The Effect of Rubber on Morphology, Thermal Properties and Mechanical Properties of PLA/NR and PLA/ENR Blends, *Energy Procedia.* 34 (2013) 888–897. doi:10.1016/J.EGYPRO.2013.06.826.
- [5] D. Sundaramurthi, U.M. Krishnan, S. Sethuraman, Electrospun nanofibers as scaffolds for skin tissue engineering, *Polym. Rev.* 54 (2014) 348–376. doi:10.1080/15583724.2014.881374.
- [6] M. Santoro, S.R. Shah, J.L. Walker, A.G. Mikos, Poly(lactic acid) nanofibrous scaffolds for tissue engineering, *Adv. Drug Deliv. Rev.* 107 (2016) 206–212. doi:10.1016/J.ADDR.2016.04.019.
- [7] D. Puppi, F. Chiellini, A.M. Piras, E. Chiellini, Polymeric materials for bone and cartilage repair, *Prog. Polym. Sci.* 35 (2010) 403–440. doi:10.1016/J.PROGPOLYMSCI.2010.01.006.
- [8] J.M. Holzwarth, P.X. Ma, Biomimetic nanofibrous scaffolds for bone tissue engineering, *Biomaterials.* 32 (2011) 9622–9629. doi:10.1016/J.BIOMATERIALS.2011.09.009.
- [9] X. Zhang, Y. Lu, Centrifugal spinning: An alternative approach to fabricate nanofibers at high speed and low cost, *Polym. Rev.* 54 (2014) 677–701. doi:10.1080/15583724.2014.935858.
- [10] J. Rogalski, C. Bastiaansen, T. Peijs, PA6 Nanofibre Production: A Comparison between Rotary Jet Spinning and Electrospinning, *Fibers.* 6 (2018) 37. doi:10.3390/fib6020037.
- [11] A.F. Pattaro, Síntese, Caracterização e Processamento de Polímeros Biorreabsorvíveis para uso na Engenharia de Tecidos (Tissue Engineering); Thesis (PhD degree), Sch. Chem. Eng. – Univ. Campinas, Campinas. (2016).
- [12] T.A.V. DE BRITO, Preparação e Caracterização de Nanofibras da Blenda PLLA/PCL obtidas pelos Processos de Eletrospinning e Rotofiação; Thesis (PhD degree), Sch. Chem. Eng. – Univ. Campinas, Campinas. (2013) 108.
- [13] and K.K.P. Mohammad Reza Badrossamay, Holly Alice McIlwee, Josue A. Goss, Nanofiber Assembly by Rotary Jet-Spinning, *Nano Lett.* 10 (2010) 2257–2261. doi:10.1038/ki.2009.479.Commonly.

- [14] S.J. Upson, T. O'Haire, S.J. Russell, K. Dalgarno, A.M. Ferreira, Centrifugally spun PHBV micro and nanofibres, *Mater. Sci. Eng. C.* 76 (2017) 190–195. doi:10.1016/j.msec.2017.03.101.
- [15] A.M. Loordhuswamy, V.R. Krishnaswamy, P.S. Korrapati, S. Thinakaran, G.D.V. Rengaswami, Fabrication of highly aligned fibrous scaffolds for tissue regeneration by centrifugal spinning technology, *Mater. Sci. Eng. C.* 42 (2014) 799–807. doi:10.1016/J.MSEC.2014.06.011.
- [16] B.E. CIOCCA, Produção, Caracterização E Avaliação in Vitro De Membranas Fibrosas De Poli (L-Ácido Láctico) (Plla) Fabricadas Por Rotofiação Para Engenharia De Tecidos., (2017) 1–80.
- [17] R. Hamid, Y. Rotshteyn, L. Rabadi, R. Parikh, P. Bullock, Comparison of alamar blue and MTT assays for high through-put screening, *Toxicol. Vitro.* 18 (2004) 703–710. doi:10.1016/J.TIV.2004.03.012.